AMERICAN SOCIETY FOR MICROBIOLOGY | mBio®

OBSERVATION

Human Papillomavirus Type 16 Circular RNA Is Barely Detectable for the Claimed Biological Activity

Lulu Yu,[a] Zhi-Ming Zheng[a]

[a]Tumor Virus RNA Biology Section, HIV Dynamics and Replication Program, Center for Cancer Research, National Cancer Institute, National Institutes of Health, Frederick, Maryland, USA

ABSTRACT Human papillomavirus type 16 (HPV16) E7 oncoprotein plays an essential role in cervical carcinogenesis and is encoded predominantly by an E6*I mRNA through alternative RNA splicing of a P97 promoter-transcribed bicistronic E6E7 pre-mRNA. Recently, an HPV16 circular RNA, circE7, was detected in two HPV16-positive cervical cancer cell lines, CaSki and SiHa. It was generated through back-splicing of the E6E7 pre-mRNA. The reported findings showed that, because viral E6*I RNA was nuclear, E7 was mainly translated from the cytoplasmic circE7, and knockdown of circE7 in CaSki cells led to reduction of E7 oncoprotein, cell proliferation, and xenograft tumor formation. We have reanalyzed the published data, conducted detailed experiments, and found that the circE7 in CaSki cells is only 0.4 copies per cell, which is ~1,640-fold lower than E6*I RNA and also barely detectable from two W12 subclone cell lines, 20861 (integrated HPV16) and 20863 (extrachromosomal HPV16) cells derived from a low-grade cervical lesion. We also determined HPV16 E6*I and E6*II RNAs in CaSki cells are mainly cytoplasmic in cell fractionation analyses, as reported in other studies. We further demonstrated that the claimed circE7 functions in the published report have resulted from off-target effects on E6*I RNA by the circE7 small interfering RNAs used in the reported study.

IMPORTANCE RNA back-splicing is a rare splicing event accounting for <1% of canonical RNA splicing and, thus, is thought to have little or no biological significance. Recently, circular RNAs (circRNAs) from RNA back-splicing have been found widely in cells and tissues and may have a role in modulating RNA transcription, splicing, and interference and antiviral innate immunity. A recent report claimed that the predominant HPV16 E6*I RNA was nuclear and unable to encode E7. Rather, a viral circE7 was responsible for translating the oncoprotein E7 in CaSki cells, a cervical cancer cell line. However, we found that both HPV16 E6*I and circE7 RNAs in CaSki cells are primarily cytoplasmic and that the copy number of viral E6*I RNA is 656 copies per cell, whereas the viral circE7 is only 0.4 copies per cell. Most importantly, we found that the claimed circE7 function resulted from off-target effect on viral E6*I RNA by the small interfering RNA (siRNA) si-circE7 designed to knock down the back-spliced circE7 RNA.

KEYWORDS E7, HPV16, RNA splicing, circular RNA

Through interactions with multiple cellular factors, the high-risk human papillomavirus (HPV) E6 and E7 oncoproteins are responsible for disrupting cell cycle control and promoting cell proliferation and transformation activities (1, 2), as well as for regulation of expression of noncoding RNAs (3, 4). These high-risk HPVs utilize a major early promoter to transcribe early transcripts that then undergo alternative RNA splicing to generate mRNAs encoding early proteins (5, 6). Specifically, in HPV16- and HPV18-positive cervical cancer cells (7–10), the production of E6 and E7 proteins is dependent on the highly efficient alternative splicing of a bicistronic E6E7 pre-mRNA transcribed from the major early promoter P97 (Fig. 1A). The E6E7 pre-mRNA has three exons and

Editor Xiang-Jin Meng, Virginia Polytechnic Institute and State University

Address correspondence to Zhi-Ming Zheng, zhengt@exchange.nih.gov.

The authors declare no conflict of interest.

This article is a direct contribution from Zhi-Ming Zheng, a Fellow of the American Academy of Microbiology, who arranged for and secured reviews by Zefeng Wang, Professor and Director, CAS-MPG Partner Institute of Computational Biology Shanghai, China, and Xuefeng Liu, Ohio State University Wexner Medical Center.

Received 6 December 2021
Accepted 9 December 2021
Published 18 January 2022

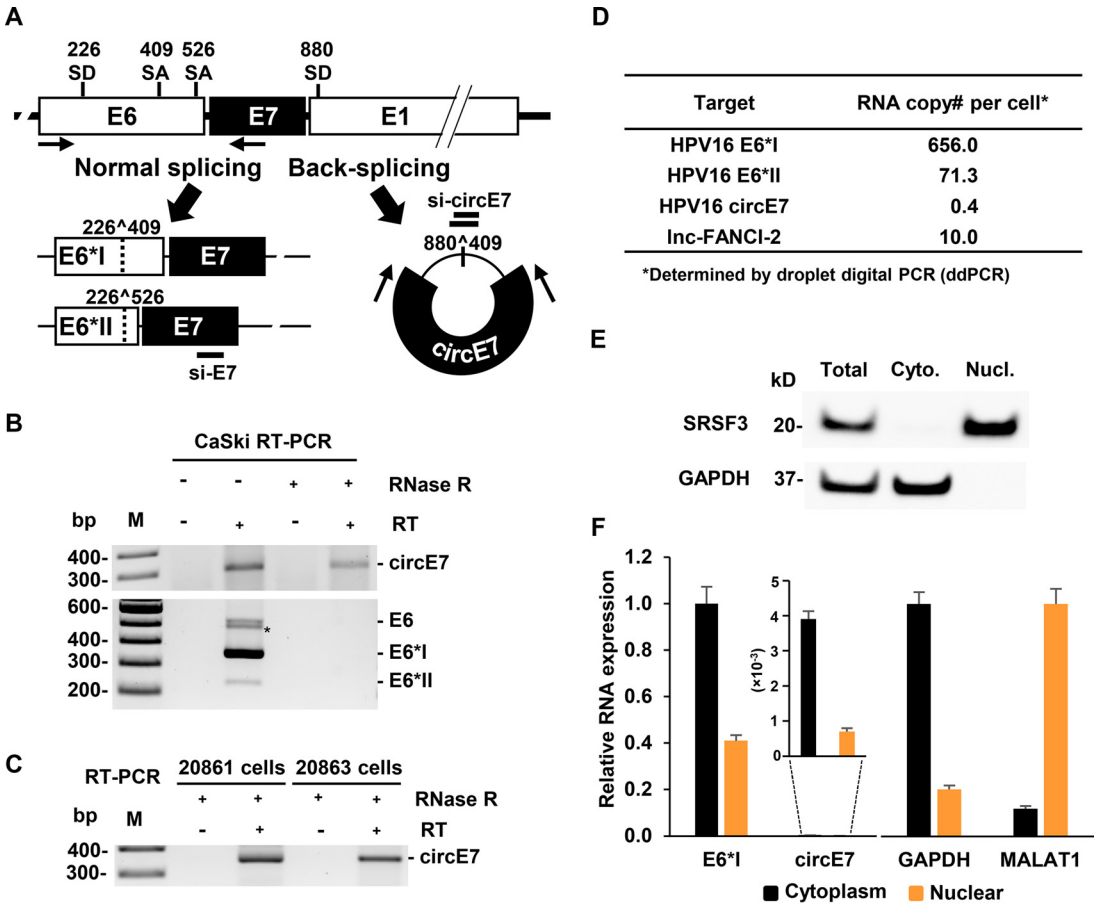

FIG 1 Characterization of HPV16 circE7 RNA expression, copy number, and localization in CaSki cells. (A) Structure diagram of viral early promoter P97-derived bicistronic HPV16 E6E7 pre-mRNA and its splicing profiles in CaSki cells. Shown on the pre-mRNA are E6, E7, and partial E1 ORF and genomic positions of viral splice donor (SD) and splice acceptor (SA) sites. Below the pre-mRNA are two spliced isoforms (E6*I and E6*II) from alternative RNA splicing commonly detected in CaSki cells and a barely detectable circE7 from back-splicing. Paired arrows below the pre-mRNA and on circE7 RNA were primers used for detection of individual products from viral RNA splicing in CaSki cells. Horizontal bars above the back-splice junctions and below the E7 ORF are siRNAs used to target circE7 (si-circE7-1 and si-circE7-2) and the corresponding RNA isoforms containing the E7 ORF region in this study. (B) Detection of HPV16 circE7 and linear E7 RNAs in CaSki cells by RT-PCR with or without RNase R treatment. RNase R (5 U)-treated total RNA (23) was reverse transcribed in a 20-μL reaction mixture, and 500 ng of the cDNA was then used for circE7 detection in 40 cycles of inverse PCR amplification, whereas 200 ng of the cDNA was used for E6*I and E6*II detection in 25 cycles of linear PCR amplification. The asterisk indicates a heteroduplex band derived from two RT-PCR products (20). (C) Detection of HPV16 circE7 in W12 subclone 20861 cells with an integrated HPV16 genome and subclone 20863 cells with an episomal HPV16 genome by RT-PCR upon RNase R treatment. RNase R (5 U)-treated total RNA was reverse transcribed in a 20 μL-reaction mixture, and 500 ng of the cDNA was then used for circE7 detection in 40 cycles of PCR amplification as described in panel B. (D) RNA copy number of the indicated HPV16 RNAs determined by ddPCR. Total cell RNA was reverse transcribed and serially diluted in triplicate before ddPCR analysis, with a long noncoding RNA lnc-FANCI-2 serving as an internal reference RNA control. (E and F) HPV16 E7 (E6*I) and circE7 RNAs in CaSki cells are predominantly cytoplasmic. (E) Nuclear and cytoplasmic fractionation efficiency was determined by immunoblot analyses of nuclear protein SRSF3 (serine and arginine rich splicing factor 3) and cytoplasmic GAPDH (glyceraldehyde-3-phosphate dehydrogenase) protein. Total fractionated cytoplasmic and nuclear RNAs were quantified, respectively, for E6*I and circE7 RNA by RT-qPCR analysis with nuclear MALAT1 (metastasis associated lung adenocarcinoma transcript 1) and cytoplasmic GAPDH RNA serving as internal controls for RNA fractionation efficiency.

two introns. Intron 1, located within the E6 open reading frame (ORF), bears one splice donor (SD) at nucleotide (nt) 226 and two major alternative splice acceptor (SA) sites, one at nt 409 and the other at nt 526. The SD site of intron 2 is located in the E1 ORF at nt 880 in the HPV16 genome and is spliced to one of several downstream SAs. Only the intron 1-retained E6E7 RNA of relatively low abundance has an intact E6 ORF capable of translating the full-length E6 protein. However, this RNA translates little or no E7 due to intercistronic space restriction because the E6 stop codon is separated from the E7 start codon by only 2 nt. This extremely short intercistronic space prevents the translating ribosome from reinitiating translation of the downstream E7 ORF after termination of E6 translation. We have previously demonstrated that the HPV16 major

spliced isoform E6*I RNA functions as an E7 mRNA for production of E7 protein (8). In this E6*I mRNA, the intron 1 splicing from nt 226 to nt 409 introduces a premature stop codon downstream of the splice junction, thereby increasing the intercistronic distance to 145 nt between the E6*I stop codon UAA and the E7 initiation codon AUG (7–9). This phenomenon also applies to HPV18 E7 production (10).

All introns in a pre-mRNA are spliced in 5′ SD to 3′ SA order as an intermediate circular lariat RNA (9, 10). Occasionally, RNA back-splicing from a downstream intron 5′ SD to an upstream intron 3′ SA over the exon(s) occurs, producing circular RNAs (circRNAs) containing the exon(s) (11). The efficiency of RNA back-splicing to produce circRNAs (Fig. 1B) is very low and accounts for $<$1% of canonical RNA splicing (12, 13). Several reports indicate that circRNAs are produced in every cell type and tissue. Because of their higher stability than mature mRNAs, it has been reported that circRNAs may act as an important modulator in regulating RNA transcription, splicing, and interference and antiviral innate immunity (11, 14–16). Recently, Zhao et al. detected a circE7 from the back-splicing of HPV16 E6E7 pre-mRNAs in CaSki and SiHa cells and in cervical cancer tissues (17). They reported that CaSki cells mainly use circE7 RNAs, not E6*I RNA, to translate E7 protein, and knocking down circE7 expression by a short hairpin RNA (shRNA)-derived small interfering RNA (siRNA) targeting the back-splice junction in CaSki cells led to reduced E7 protein expression and, subsequently, cell proliferation or xenograft tumor formation (17).

To confirm the reported circE7 findings, we conducted detailed experiments to determine the circE7 production, its subcellular localization, and copy number per cell, as well as its function, in parallel with E6*I. The circE7 RNA produced from back-splicing is predicted to be 472 nt long (Fig. 1A). We detected the production of circE7 in CaSki cells by reverse transcriptase PCR (RT-PCR) using an inverse primer pair (Table S1 in the supplemental material). This primer pair detected an expected circE7 RNA of 351 nt (Fig. 1A and B). We found that the detected circE7 RNA in CaSki cells did not appear to be enriched by RNase R treatment (Fig. 1B), contrary to the report by Zhao et al. (17). Approximate 500 ng of total cDNA and 40 cycles of inverse PCR were needed to detect circE7 RNA because of its extremely low abundance in CaSki cells (Fig. 1B) and in the two W12 subclone cell lines (Fig. 1C). In contrast, HPV16 E6*I and E6*II RNAs in CaSki cells were detected by using 200 ng of total cDNA and 25 PCR cycles (Fig. 1B). The circE7 RNA generated by RT-PCR was confirmed by Sanger sequencing.

We have been studying the RNA splicing of both HPV16 and HPV18 E6E7 pre-mRNAs and its regulation and relationship to translation of E7 proteins (7–10, 18–20). For this study, we quantified, by droplet digital PCR (ddPCR), the copy number of HPV16 E6*I, E6*II, and circE7 in CaSki cells using human lnc-FANCI-2 with a known RNA copy number per CaSki cell (4) as a reference RNA. We found only 0.4 copies of circE7 per CaSki cell, ~1,640-fold lower than E6*I RNA and 178-fold lower than E6*II (Fig. 1D). Consistent with our previous report (19), the copy number of E6*I RNA in CaSki cells was ~10 times higher than E6*II RNA. In the reported study by Zhao et al. (17), a minimal amount of circE7 RNA in CaSki cells was detected by Northern blotting. However, the reported Northern blot band of ~700-nt size was longer than the predicted circE7 RNA size of 472 nt. Furthermore, there was no additional verification of the identity of this band to be the authentic circE7.

The majority of HPV16 early transcripts and spliced RNA isoforms have previously been identified in the cytoplasm by cell fractionation and Northern blot analysis (18). Consistent with this report, we further verified that both the E6*I and circE7 RNAs in CaSki cells were primarily cytoplasmic by cell fractionation analysis (Fig. 1E and F). As expected, the level of circE7 RNA in the cytoplasm was of extremely low abundance compared to E6*I RNA (Fig. 1F). In contrast, Zhao et al. found viral linear E6*I RNA was detected predominantly in the nuclear fraction by SYBR green reverse transcriptase quantitative PCR (RT-qPCR) both in CaSki cells and in an E6E7 minigene-transfected HEK293T cell (Zhao et al., Fig. 3b) (17). To resolve this discrepancy, we then analyzed their primer sequences and found that the primer pair in Zhao's report detected only the less abundant intron 1-containing E6 RNA or, most likely, the nuclear E6E7 pre-mRNA, but not the predominant E6*I RNA in the cytoplasm of CaSki cells. It is also

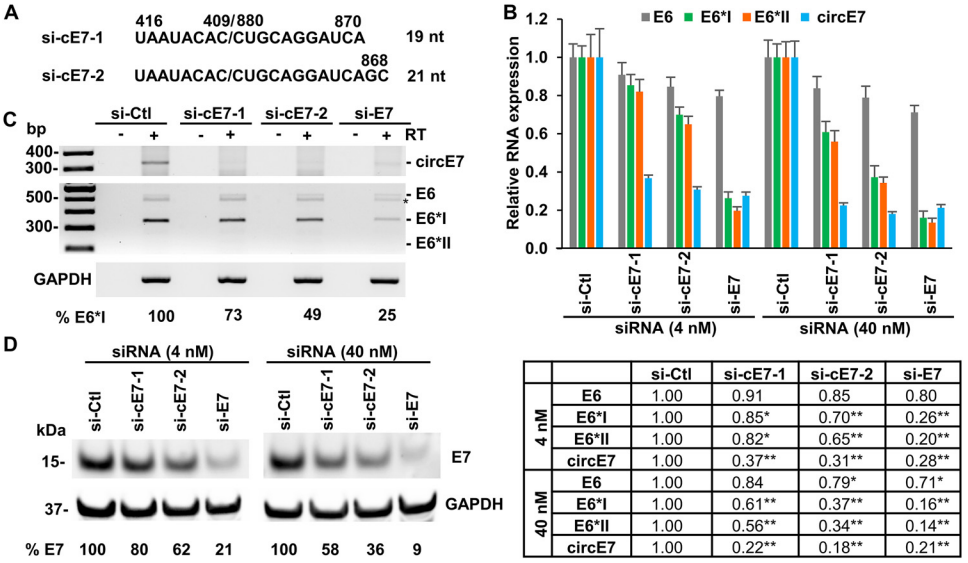

		si-Ctl	si-cE7-1	si-cE7-2	si-E7
4 nM	E6	1.00	0.91	0.85	0.80
	E6*I	1.00	0.85*	0.70**	0.26**
	E6*II	1.00	0.82*	0.65**	0.20**
	circE7	1.00	0.37**	0.31**	0.28**
40 nM	E6	1.00	0.84	0.79*	0.71*
	E6*I	1.00	0.61**	0.37**	0.16**
	E6*II	1.00	0.56**	0.34**	0.14**
	circE7	1.00	0.22**	0.18**	0.21**

FIG 2 HPV16 circE7-specific siRNAs' off-target expression of both E6*I and E6*II RNAs and E7 protein in CaSki cells. (A) Nucleotide sequences of two synthetic siRNAs targeting the circE7 back-splice junction, with si-cE7-1 standing for si-circE7-1 and si-cE7-2 for si-circE7-2. (B to D) HPV16 circE7-specific siRNAs affect the expression of both E6*I and E6*II RNAs and E7 protein in CaSki cells. Cell lysates were prepared 72 h after transfection of indicated individual siRNAs at 4 nM or 40 nM, with si-Ctl standing for nontargeting siRNA control. (B) Total RNA extracted from the cells was reverse transcribed, and the cDNAs prepared were used to quantify HPV16 E6, E6*I, E6*II, and circE7 RNAs by RT-qPCR using individual specific TaqMan probes. Data are mean ± SE of three repeats. *, $P < 0.05$; **, $P < 0.01$ by unpaired, two-tailed Student's *t* test. The relative E6*I RNA level was quantified after normalizing to GAPDH in each sample. The cDNAs were also used to profile the effects of individual siRNAs on viral circE7, bicistronic E6E7 RNA, and spliced E6*I RNA by RT-PCR and agarose gel electrophoresis. (C) A total of 500 ng cDNA and 40 cycles of PCR were used to detect circE7, and 100 ng of cDNA and 25 cycles of PCR were used to detect the unspliced E6E7 and spliced E6*I RNAs and the cellular GAPDH pre-mRNAs, which served as the RNA loading control. E6*II was not detectable at 100 ng of cDNA and 25 cycles of PCR. The asterisk indicates a heteroduplex band derived from two RT-PCR products (20). Total cell lysates were also immunoblotted for E7 protein expression by an anti-HPV16 E7 antibody. (D) The relative E7 protein level in each sample was quantified after normalizing with GAPDH serving as the protein loading control, with E7 level in the siRNA control (si-Ctl) sample as 100.

difficult to determine the exact amount of linear E6*I RNA that was expressed from each minigene in HEK293 cells by SYBR green RT-qPCR, as all data in Zhao's report were shown as a ratio (Zhao et al., Fig. 3b); only the circE7 RNA was displayed in Northern blots (Zhao et al., Fig. 3a) (17).

We then investigated how the circE7 RNA at such a low level in CaSki cells could exhibit the high impact on E7 production and activities in cell proliferation and xenograft tumor formation reported by Zhao et al. (17). We designed two siRNAs targeting the back-splice junction of HPV16 circE7 RNA (Fig. 2A), with si-circE7-2 being identical to the circE7-sh2-derived siRNA sequence in the Zhao et al. study (17). After delivery of the siRNAs to CaSki cells, we found, by quantitative TaqMan RT-qPCR (Fig. 2B), that both si-circE7-1 and si-circE7-2 at 4 nM knocked down circE7 RNA by ~60 to 70% and at 40 nM by ~80%, but si-circE7-1 also reduced E6*I and E6*II RNAs by ~15 to 18% at 4 nM and by ~40% at 40 nM. The si-circE7-2, which is 2 nt longer than si-circE7-1, decreased E6*I and E6*II RNA up to ~30 to 35% at 4 nM and ~65% at 40 nM, whereas si-E7 targeting the E7 ORF region (8) inhibited the expression of E6*I, E6*II, and circE7 RNAs by ~70 to 80% at 4 nM and ~80% at 40 nM. We also found that all three siRNAs affected the expression of the unspliced viral E6 RNAs by 10 to 20% at 4 nM and by ~16 to 30% at 40 nM (Fig. 2B). Splicing profile analysis by RT-PCR and agarose gel electrophoresis confirmed the siRNA knockdown effects on both circE7 and E6*I RNAs (Fig. 2C). Immunoblot analyses of the siRNA-treated CaSki cells further confirmed these three siRNA-mediated reductions of E7 protein expression in a dose-dependent manner and in the order of si-E7 > si-circE7-2 > si-circE7-1 (Fig. 2D). The data are striking because we found that si-circE7-2 with 13-nt sequence overhang to the back-splice

junction had a bigger off-target effect on linear E6*I and E6*II RNAs than si-circE7-1 with the 11-nt overhang sequence.

Although Zhao et al. claimed that their shRNA-derived siRNAs had no effects on linear E6/E7 or E6*I RNAs in CaSki cells (17), lack of an internal RNA loading control and probe information in the Northern blotting (Zhao et al., Fig. S4b) and the calculation of the effects of circE7 shRNAs on E6*I RNA by the unusual normalization to β-actin in the SYBR green RT-qPCR (Zhao et al., Fig. S4c) (17) raised a red flag for their data interpretation. We also question why two siRNAs targeting the linear E6*I RNA expressed from the minigenes in Zhao's report led to its RNA reduction by $\geq$75% (Zhao et al., Fig. S3e) but did not decrease the expression of FLAG-E7 protein (Zhao et al., Fig. 2c) (17). In fact, addition of the QKI binding site to facilitate the circulation of E6E7 RNA in the reporter minigene only enhanced circE7 production by 2-fold (Zhao et al., Fig. S3c). This small increase of circE7 production should not significantly affect the vast amount of production of E6*I from the minigene vector. Unless a complete E6E7 expression profile is provided from the transfected minigene, it would be difficult to conclude that E7 protein was only translated from circE7, not from linear E6*I RNA. Clearly, the authors imply that their linear E6*I RNA in CaSki and minigene-transfected HEK293T cells somehow did not translate E7 protein because of its primary nuclear localization in their report (17). But their conclusion was not supported by our experimental results.

By examination of the published wild-type E7 sequence (Zhao et al., Data Set S2), we found, surprisingly, that the so-called circE7 g-block wild-type sequence in Zhao's study (17) had four AUG mutations, including the AUG mutation for E7 translation when aligned against the HPV16 reference genome (Fig. S1 in our report). It is obvious from the deposited Data Set S2 that the minigene plasmids used in Zhao's report were messed up, and it is impossible to tell which plasmid was used for what experiment. As Zhao's shRNA study cannot unequivocally prove that E7 protein is produced only from the circE7 in CaSki cell, we believe that the claimed circE7 function in E7 protein production responsible for E7 activities was attributable to the off-target effects of their si-circE7s on E6*I RNA.

Strikingly, Zhao's report (17) utilized unconventional HPV16 genome positions (Zhao et al., Fig. 1 and Fig. S1) to describe their circE7 production and viral RNA splicing, thereby making it difficult for HPV virologists to follow from the very beginning of their report. Because this is in contrast to the conventional numbering system in the papillomavirus field, we had to align their HPV16 genome sequence and positions to an HPV16 reference genome from the papillomavirus database PAVE (http://pave.niaid.nih.gov) in order to understand how their studies were designed and performed. Zhao's report (17) is also difficult to follow because of mislabeled figure panels (Zhao et al., Fig. S2b, Fig. 2c, Fig. 4a, and Fig. 5a and b), a missing figure legend (Zhao et al., Fig. S5f), lack of size marker labels for RT-PCR products (Zhao et al., Fig. 1d, Fig. 2b and e, Fig. 3g, Fig. 5d and e, Fig. S2c, and Fig. S3c and g) and Northern blots (Zhao et al., Fig. S2b and Fig. S4b), and lack of appropriate controls.

Seeking a functional circRNA has been a major focus in the modern RNA world. Although the production of circRNA has resulted from a rare RNA back-splicing event, the nature of circular form makes this species of the RNA resistant to cellular exonuclease digestion and, thus, more stable than linear mRNA. In this report, we confirmed the production, though barely detectable, of HPV16 circE7 RNA in a cervical cancer cell line, CaSki cells, and also in two W-12 subclone cell lines derived from a low-grade cervical lesion. We quantitatively determined the presence of only 0.4 copies of the circE7 RNA per CaSki cell, whereas the copy number/per cell of E6*I RNA is 656, $\sim$1,640-fold higher. We also determined both RNAs were primarily located in the cytoplasm. It is difficult to ascribe a critical biological function claimed by Zhao et al. (17) to this extremely low abundance of the circE7 RNA (17). Moreover, although a circRNA bearing an internal ribosome entry site (IRES), but lacking a 5′ cap, might be translatable (21, 22), HPV16 E7 ORF does not have a conventional IRES, and thus, the circE7 RNA derived from this region cannot elicit a cap-independent translation of E7 protein. Finally, we found the siRNA si-circE7 targeting the circE7 back-splicing junction exhibits

a severe off-target effect on the cytoplasmic E6*I RNA, which functions as a true E7 mRNA (8, 9). On the basis of all the data that we presented here, we concluded that the claimed circE7 RNA functions in Zhao's report (17) are attributed to the off-target effects of the si-circE7 on E6*I RNA. The reduction of E6*I and E6*II RNAs and reduced E7 protein would certainly account for the decreased cell proliferation and tumorigenesis in nude mice reported by Zhao et al. in their circE7 knockdown experiments (17).

SUPPLEMENTAL MATERIAL

Supplemental material is available online only.

TEXT S1, DOCX file, 0.02 MB.

FIG S1, TIF file, 1.1 MB.

TABLE S1, XLSX file, 0.01 MB.

ACKNOWLEDGMENTS

We thank Louise Chow for her critical comments, Anne Arthur for proofreading of our manuscript, and Xiaolin Wu and David Sun of Frederick National Laboratory for Cancer Research for ddPCR analysis. We also thank other members of the Zheng lab for comments and suggestions in the course of this study.

This study was supported by the Intramural Research Program of the National Institutes of Health, National Cancer Institute, Center for Cancer Research (ZIASC010357 to Z.M.Z.).

We declare no competing interests.

REFERENCES

1. Vande Pol SB, Klingelhutz AJ. 2013. Papillomavirus E6 oncoproteins. Virology 445:115–137. https://doi.org/10.1016/j.virol.2013.04.026.
2. Roman A, Munger K. 2013. The papillomavirus E7 proteins. Virology 445:138–168. https://doi.org/10.1016/j.virol.2013.04.013.
3. Wang X, Wang HK, Li Y, Hafner M, Banerjee NS, Tang S, Briskin D, Meyers C, Chow LT, Xie X, Tuschl T, Zheng ZM. 2014. microRNAs are biomarkers of oncogenic human papillomavirus infections. Proc Natl Acad Sci U S A 111:4262–4267. https://doi.org/10.1073/pnas.1401430111.
4. Liu H, Xu J, Yang Y, Wang X, Wu E, Majerciak V, Zhang T, Steenbergen RDM, Wang HK, Banerjee NS, Li Y, Lu W, Meyers C, Zhu J, Xie X, Chow LT, Zheng ZM. 2021. Oncogenic HPV promotes the expression of the long noncoding RNA lnc-FANCI-2 through E7 and YY1. Proc Natl Acad Sci U S A 118:e2014195118. https://doi.org/10.1073/pnas.2014195118.
5. Zheng ZM, Baker CC. 2006. Papillomavirus genome structure, expression, and post-transcriptional regulation. Front Biosci 11:2286–2302. https://doi.org/10.2741/1971.
6. Johansson C, Schwartz S. 2013. Regulation of human papillomavirus gene expression by splicing and polyadenylation. Nat Rev Microbiol 11:239–251. https://doi.org/10.1038/nrmicro2984.
7. Zheng ZM, Tao M, Yamanegi K, Bodaghi S, Xiao W. 2004. Splicing of a cap-proximal human Papillomavirus 16 E6E7 intron promotes E7 expression, but can be restrained by distance of the intron from its RNA 5' cap. J Mol Biol 337:1091–1108. https://doi.org/10.1016/j.jmb.2004.02.023.
8. Tang S, Tao M, McCoy JP, Jr., Zheng ZM. 2006. The E7 oncoprotein is translated from spliced E6*I transcripts in high-risk human papillomavirus type 16- or type 18-positive cervical cancer cell lines via translation reinitiation. J Virol 80:4249–4263. https://doi.org/10.1128/JVI.80.9.4249-4263.2006.
9. Ajiro M, Jia R, Zhang L, Liu X, Zheng ZM. 2012. Intron definition and a branch site adenosine at nt 385 control RNA splicing of HPV16 E6*I and E7 expression. PLoS One 7:e46412. https://doi.org/10.1371/journal.pone.0046412.
10. Brant AC, Majerciak V, Moreira MAM, Zheng ZM. 2019. HPV18 utilizes two alternative branch sites for E6*I splicing to produce E7 protein. Virol Sin 34:211–221. https://doi.org/10.1007/s12250-019-00098-0.
11. Li X, Yang L, Chen LL. 2018. The biogenesis, functions, and challenges of circular RNAs. Mol Cell 71:428–442. https://doi.org/10.1016/j.molcel.2018.06.034.
12. Pasman Z, Been MD, Garcia-Blanco MA. 1996. Exon circularization in mammalian nuclear extracts. RNA 2:603–610.
13. Barrett SP, Wang PL, Salzman J. 2015. Circular RNA biogenesis can proceed through an exon-containing lariat precursor. Elife 4:e07540. https://doi.org/10.7554/eLife.07540.
14. Kristensen LS, Andersen MS, Stagsted LVW, Ebbesen KK, Hansen TB, Kjems J. 2019. The biogenesis, biology and characterization of circular RNAs. Nat Rev Genet 20:675–691. https://doi.org/10.1038/s41576-019-0158-7.
15. Liu CX, Li X, Nan F, Jiang S, Gao X, Guo SK, Xue W, Cui Y, Dong K, Ding H, Qu B, Zhou Z, Shen N, Yang L, Chen LL. 2019. Structure and degradation of circular RNAs regulate PKR activation in innate immunity. Cell 177:865–880.e21. https://doi.org/10.1016/j.cell.2019.03.046.
16. Zheng ZM. 2019. Circular RNAs and RNase L in PKR activation and virus infection. Cell Biosci 9:43. https://doi.org/10.1186/s13578-019-0307-x.
17. Zhao J, Lee EE, Kim J, Yang R, Chamseddin B, Ni C, Gusho E, Xie Y, Chiang CM, Buszczak M, Zhan X, Laimins L, Wang RC. 2019. Transforming activity of an oncoprotein-encoding circular RNA from human papillomavirus. Nat Commun 10:2300. https://doi.org/10.1038/s41467-019-10246-5.
18. Jia R, Liu X, Tao M, Kruhlak M, Guo M, Meyers C, Baker CC, Zheng ZM. 2009. Control of the papillomavirus early-to-late switch by differentially expressed SRp20. J Virol 83:167–180. https://doi.org/10.1128/JVI.01719-08.
19. Ajiro M, Zheng ZM. 2015. E6^E7, a novel splice isoform protein of human papillomavirus 16, stabilizes viral E6 and E7 oncoproteins via HSP90 and GRP78. mBio 6:e02068-14–e02014. https://doi.org/10.1128/mBio.02068-14.
20. Ajiro M, Tang S, Doorbar J, Zheng ZM. 2016. Serine/arginine-rich splicing factor 3 and heterogeneous nuclear ribonucleoprotein A1 regulate alternative RNA splicing and gene expression of human papillomavirus 18 through two functionally distinguishable cis elements. J Virol 90:9138–9152. https://doi.org/10.1128/JVI.00965-16.
21. Yang Y, Fan X, Mao M, Song X, Wu P, Zhang Y, Jin Y, Yang Y, Chen LL, Wang Y, Wong CC, Xiao X, Wang Z. 2017. Extensive translation of circular RNAs driven by N(6)-methyladenosine. Cell Res 27:626–641. https://doi.org/10.1038/cr.2017.31.
22. Chen CK, Cheng R, Demeter J, Chen J, Weingarten-Gabbay S, Jiang L, Snyder MP, Weissman JS, Segal E, Jackson PK, Chang HY. 2021. Structured elements drive extensive circular RNA translation. Mol Cell 81:4300–4318.e13. https://doi.org/10.1016/j.molcel.2021.07.042.
23. Suzuki H, Zuo Y, Wang J, Zhang MQ, Malhotra A, Mayeda A. 2006. Characterization of RNase R-digested cellular RNA source that consists of lariat and circular RNAs from pre-mRNA splicing. Nucleic Acids Res 34:e63. https://doi.org/10.1093/nar/gkl151.